Gamma Imaging with Negatively Charge-Modified Monoclonal Antibody: Modification with Synthetic Polymers

Ban-An Khaw, Alexander Klibanov, Sean M. O'Donnell, Tomiyoshi Saito, Naseem Nossiff, Mikhail A. Slinkin, John B. Newell, H. William Strauss, and Vladimir P. Torchilin

Division of Nuclear Medicine and Cardiac Unit, Massachusetts General Hospital, Boston, Massachusetts, and Institute of Experimental Cardiology, Moscow, Soviet Union

Antimyosin Fab has been modified to carry highly negatively charged synthetic polymers containing DTPAs (DTPA-PL) as chelating agents, of starting molecular weights 3.3 and 17 kD. The immunoreactivities of the modified antibodies were unaffected by the modification procedure. The isoelectric points (PI) of unmodified antimyosin (AM) Fab (PI range 7–9, M_r = 52kD) were changed to PIs predominantly between 4 and 5 (M_r = 59 kD for DTPA-$PL_{3.3kD}$-AM-Fab and 67kD for DTPA-PL_{17kD}-AM-Fab). These AM-Fab preparations were tested for specific target localization and visualization in vivo in an experimental canine model of acute myocardial infarction. The charge-modified ^{111}In-labeled AM-Fab preparations showed enhanced target (necrotic myocardium) visualization within 30 min of intravenous infusion and decreased background activity in normal myocardium (mean %ID/g ± s.e.m., 0.0076 ± 0.0006, n = 164, and 0.0056 ± 0.0004, n = 92, for ^{111}In-DTPA-$PL_{3.3kD}$- and DTPA-PL_{17kD}-AM-Fab respectively) relative to conventional ^{111}In-DTPA-AM-Fab (0.0263 ± 0.0037, n = 135) ($p < 0.001$) or radioiodinated AM-Fab (0.0098 ± 0.0006, n = 256) ($p \leq 0.001$). Furthermore, the concentration of negatively charged ^{111}In-labeled antimyosin Fab decreased in non-target organs such as the liver and kidneys. In diagnostic and therapeutic applications, charge-modified macromolecules may improve target localization and reduce non-target organ activity.

J Nucl Med 1991; 32:1742–1751

Membrane surface-bound acidic residues give mammalian cells their negative charge (zeta potential) (*1–3*). Antibodies, on the other hand, are basic, positively charged proteins (*4*). Although the primary effect of antibodies is through their interaction with antigen-specific binding sites, antibodies also interact with other in vivo structures by electrostatic bonding. Radiolabeled antibody imaging appears to be hindered by high non-target organ sequestration of the radioactivity. High liver and kidney activities are observed with radiolabeled antibodies and more so with fragments of the antibodies in the kidneys. This nonspecific interaction most probably decreases contrast between target (antigen-specific binding sites) and background. We hypothesized that negatively charged antibody molecules would enhance specific interaction by decreased nonspecific (background) activity.

Monoclonal antimyosin Fab labeled with ^{111}In (^{111}In-AM-Fab) has been used for the noninvasive diagnosis of acute myocardial infarction, heart transplant rejection, and acute myocarditis (*5–9*). Indium-111-AM-Fab is a sensitive and specific delineator of myocardial necrosis that localizes to its target site (myosin exposed after myocardial cell death) immediately after intravenous administration. However, 18–48 hr must pass before a lesion can be visualized, because it takes that long for the antibody activity to clear from the blood pool and normal myocardium. Additional visualization problems stem from high concentrations of antibody in the liver and kidneys, which can interfere with the detection of lesions in the inferior wall of the myocardium and limit the dose of ^{111}In that can be safely administered to the patient.

We previously reported that a negatively charged synthetic polymer (DTPA-succinylated polylysine 14 kD) could be coupled to AM-Fab without reducing its immunoreactivity (*10*). In biodistribution studies in normal mice (that is, without specific target organs), negatively charged AM-Fab showed similar blood clearance but reduced hepatic and renal concentrations in comparison with conventional ^{111}In-AM-Fab. To determine whether negatively charged AM-Fab could accelerate visualization of a specific target such as necrotic myocardium, we performed the present study in a canine model of myocardial infarction. An improved method of covalent-linkage of negatively charged polymers to antimyosin Fab is also described. The results were also compared to the radioiodinated antimyosin Fab, since the liver and kidney activities of radioiodine labeled antibodies are known to be substantially less than the radio-metal chelate labeled antibodies due to in vivo dehalogenation.

Received Jan. 28, 1991; revision accepted Mar. 27, 1991.

For reprints contact: Ban An Khaw, PhD, Massachusetts General Hospital-East, Radiology Laboratory, Rm. 5410, Bldg. 149, 13th St., Charlestown, MA 02129.

METHODS

Monoclonal antimyosin antibody R11D10 and its Fab fragments were prepared as previously described (*11*). Antimyosin Fab covalently linked with DTPA by the bicyclic anhydride method (*12*) was supplied by Centocor (Malvern, PA).

Modification of Polylysine (PL 3.3 kD and 17 kD)

Preparation of Acidic Polymer. Polylysine (PL) with average molecular weights of 3.3 and 17 kD were obtained from Sigma. DTPA was covalently linked to PL (3.3 or 17 kD) by the mixed anhydride method of Krejcarek and Tucker (*13*) as described previously (*10*). To an aliquot of 10–20 mg PL per ml in 0.1 *M* $NaHCO_3$, aliquots of 10% by volume of mixed anhydride of DTPA (50 mg/ml) were added with continuous stirring. For optimal substitution with DTPA, five additions of the anhydride were applied, followed by complete succinylation of the residual free epsilon amino groups of the lysyl residues by addition of a 10-fold molar excess of succinic anhydride (with respect to total amino groups of the PL) in 0.1 *M* $NaHCO_3$. Completion of the substitution was followed by reaction of an aliquot of the polymer with trinitrobenzene-sulfonic acid (*14*). No color reaction was achieved with completely succinylated PL. Approximately 30%–50% of total lysyl residues of the polylysine were assessed to be modified with DTPA by determination of the percent binding of tracer ^{111}In-citrate in a known concentration of cold ^{111}In-citrate (~0.25 μmole).

Covalent Coupling of Acidic PL to Antibody. Covalent coupling of the DTPA-succinylated polylysine (DTPA-PL) to AM-Fab was achieved by modification of the water soluble carbodiimide protocol previously described (*10*) by using an intermediary carrier, n-hydroxy sulfosuccinimide (n-HSS) (*15*). DTPA-PL 3.3 kD or 17 kD at 8.33×10^{-5} mmol (333 μg) in 250 μl distilled deioinized H_2O (pH adjusted to 4.0) was mixed with 14-fold molar excess (1.15×10^{-3} mmol) of n-HSS (250 μg/250 μl) in deionized distilled H_2O. To this, approximately 400 μg/40 μl 1-ethyl-3-(3-dimethylamino-propyl) carbodiimide (EDC) (9.4 mg/ml) were added and immediately followed by another aliquot of n-HSS. The reaction was allowed to proceed at room temperature for 5 min. Free n-HSS and EDC were separated from n-sulfosuccinylated-DTPA-PL by Sephadex-G25 column centrifugation. The smaller n-HSS and free EDC remain in the column, whereas, the n-sulfosuccinylated DTPA-PL was directly eluted into receptacles containing 1 mg AM-Fab in 1 ml of 0.1 *M* borate (pH 8.3). This procedure reduced the amount of denaturation and polymerization which might be affected by the reaction of excess free EDC with AM Fab.

Purification of DTPA-PL-AM-Fab from Free DTPA-PL and AM-Fab. DTPA-PL-AM-Fab was separated from free DTPA-PL and AM-Fab by DEAE Sephadex A-25 (Sigma) anion-exchange column chromatography. A 5–10-ml column of DEAE Sephadex A-25 was equilibrated in 0.05 *M* phosphate buffer (pH 6.0). The reaction mixture was loaded on the column and eluted with 3 column volumes of equilibrating buffer. Free Fab was eluted in the wash. DTPA-PL-AM-Fab was eluted from the column with 0.45 *M* NaCl step gradient, whereas free DTPA-PL was eluted from the column by a 0.95 *M* NaCl step gradient. The peak tubes containing DTPA-PL-AM-Fab were pooled, and the antibody concentration was estimated from the optical density reading at 280 nm utilizing an extinction coefficient of 1.5 for Fab.

Verification of DTPA-$PL_{3.3\ or\ 17kD}$-AM-Fab. The three peaks obtained following anion-exchange chromatography were assessed by SDS-PAGE, Western blot, their capacity to chelate ^{111}In and by radioimmunoassay for direct binding of ^{111}In-labeled preparations.

Determination of Immunoreactivity

Immunoreactivity was determined by comparison of the apparent affinities (K_a) of the various preparations of AM-Fab by solid-phase radioimmunoassay (*11*). K_a were calculated by the method of van Heyningen et al. (*16*) at 50% of maximal binding of the antibody. Serial dilutions of the modified antimyosin were compared to serial dilutions of unmodified and conventionally DTPA-modified antimyosin Fab. Briefly, Cook's microtiter wells were coated with 50 μl of 10 μg/ml solution of human cardiac myosin, then the plates were blocked and washed 12 times with 1% horse serum in 0.15 *M* phosphate buffered saline (pH 7.4). Duplicate samples of 50-μl aliquots of the serial dilutions of the antimyosin preparations were then added to each well and incubated eitehr at room temperature for 3 hr or at 4°C overnight. Serial dilutions of antibody concentration ranged grom 0.1 ng to 100 μg. The antibody was then removed, and the wells were again washed 12 times with 1% horse serum in 0.15 *M* phosphate-buffered saline (PBS). The 50-μl aliquots of 50,000 cpm of ^{125}I-labeled goat anti-murine IgG Fab (GAM-Fab) were added to the wells and incubated at room temperature for 1–2 hr. The excess radioactivity was removed from each well by aspiration into a radioactive waste container, followed by washing 12 times with 1% HS-PBS. The wells were cut out and counted in a gamma scintillation counter for the 30 and 60 keV peaks of ^{125}I (Micromedics gamma counter). Counts per minute of ^{125}I activity bound to each well (y-axis) was plotted against the antibody concentration (x-axis).

Radiolabeling

Radioiodination. GAM-Fab was labeled with ^{125}I by the chloramine-T method (*17*). Free and bound ^{125}I was separated by column chromatography using a 10-ml Sephadex-G25 column. Iodine-125-labeled GAM-Fab eluted in the void volume was pooled and stored frozen in 1% bovine serum albumin until used.

Radioiodination. Iodine-123 and ^{125}I were radiolabeled to AM-Fab by the iodogen iodination method (*18*). Free and antimyosin-bound radioactivity were separated as described above.

Indium-111 Labeling. DTPA-PL-coupled antimyosin Fab was labeled with ^{111}In by the transchelation method utilizing 0.1 to 0.5 *M* citrate (pH 5.5) as the weak transchelator (*19*). Indium-111-Cl_3 (37.5 MBq) was added to an equi-volume of 1 *M* citrate (pH 5.5), then 10–20 μg of DTPA-PL (3.3 or 17 kD) AM-Fab in 0.05 *M* PBS were added to the ^{111}In-citrate solution. The transchelation is allowed to proceed for 15 min, then bound and free ^{111}In were separated by Sephadex-G25 column chromatography.

In later labeling of DTPA-PL_{17kD} AM-Fab of about 10–20 μg aliquots, the antibody sample was added to 1 mg of carrier crystalline BSA (or another homologous carrier protein such as HSA for clinical use) prior to addition of ^{111}In-citrate to minimize denaturation and loss through adsorption to test tube surfaces and column matrix of a very dilute solution of the antibody. Radiolabeling of DTPA-AM-Fab with ^{111}In was as previously reported (*5*).

Electrophoresis

Isoelectrofocusing using an LKB Multiphor isoelectrofocusing apparatus was performed on DTPA-$PL_{3.3}$-, PL_{17kD}-AM Fab, DTPA-AM-Fab, and unmodified AM-Fab to determine the iso-

electric points of these preparations (*20*). Standards with isoelectric points ranging between 3.5 and 9.3 were used to calibrate the PIs of the samples.

Homogeneity of the polymer-modified antimyosin Fab was determined by 7.5% SDS polyacrylamide gel electrophoresis in non-reducing condition (*21*), and the molecular weights were assessed by comparison to M_r standards of 14.4, 20.1, 30, 43, 67, and 97 kD. The M_r of the samples were estimated by comparison to the Rf (relative mobility) values of the standards.

Experimental Protocol

Twenty-six mongrel dogs were used in this study. Four dogs were lost due to ventricular fibrillation and were excluded from the study. The remaining animals were divided into two study groups of six each for ^{111}In-DTPA-$PL_{3.3kD}$ and -PL_{17kD}-AM-Fab, one group of seven dogs as controls with ^{111}In-DTPA AM-Fab and one group of three dogs injected with ^{111}In-labeled DTPA-$PL_{3.3kD}$ as a negative control. Two dogs from the group injected with ^{111}In-DTPA-PL_{17kD}-AM-Fab were excluded from the calculations due to a modification in ^{111}In labeling protocol to reduce the hepatic activity (described below).

Dogs were anesthetized by intravenous administration of 30 mg/kg sodium pentobarbitol, and respiration was maintained on room air using a Harvard Respirator. A left thoracotomy was performed through the fifth intercostal space, and the heart was suspended in a pericardial cradle. A segment of the left anterior descending coronary artery (LAD), approximately two-thirds the distance from apex to base, was isolated and a silk ligature was placed around the segment. The right femoral artery was also isolated and a pressure transducer was attached to monitor arterial pressure. The femoral vein was cannulated for taking blood samples. Intravenous lines were established in the brachial vein of the right foreleg. For subsequent histochemical confirmation of acute myocardial infarction, an atrial line for the administration of triphenyltetrazolium chloride was inserted into the left atrial appendage. The LAD was occluded for 3 hr before blood flow was restored by removal of the occlusive ligature (*11*). Fifteen minutes after reperfusion, 22.5 MBq of ^{201}Tl was administered intravenously, and, after another 15 min, ^{201}Tl distribution images (at the 80 keV photopeak with a 20% window) were obtained in the left lateral position to confirm myocardial perfusion deficit. Immediately after ^{201}Tl imaging a bolus of a mixture of approximately 30 MBq ^{111}In-labeled DTPA-$PL_{(3.3\text{ or }17kD)}$-AM-Fab (~8 μg each, n = 6 for each group) and 15 MBq of radioiodine-labeled antimyosin Fab (^{125}I, n = 7, or ^{123}I, n = 5) in lactate ringers solution was injected intravenously. A series of 60-sec acquisition images was obtained for the next 64 min (at the 247 keV, higher energy peak of ^{111}In, with a 20% window). Hourly images were obtained for the next 4 hr. Blood samples were also obtained at 1, 2, 3, 5, 10, 15, 30, 45, 60, 75, 90, 120, 150, 180, 210, and 240 min after administraiton of the ^{111}In-labeled reagents. The 1-min blood sample served as the 100% blood activity reference standard. After gamma imaging at 4 hr, the animals were killed by overdose pentobarbitol anesthesia and intra-atrial infusion of warm (~40°C) 2% triphenyltetrazolium chloride (200 ml). The heart, lungs, liver, spleen, kidneys (cortex and medulla), abdominal skeletal muscles, and intestine were excised and weighed, and organ pieces of approximately 1 g were counted in a gamma counter for ^{201}Tl, ^{111}In, and radioiodine distributions. The heart was imaged whole and as 1-cm bread-loaf slices for ^{201}Tl, ^{111}In, and radioiodine activities. When ^{123}I-labeled AM-Fab was used in the study, a photopeak of 159 keV with a 20% window was employed. However, when ^{125}I-labeled AM-Fab was used, the x-ray peak of ^{125}I was used to image the iodine distribution. Following imaging, the heart slices were cut into endocardial and epicardial pieces of approximately 1 g, weighed, and counted in a gamma counter (Compugamm, LKB) for radioiodine, ^{111}In and ^{201}Tl activities. Aliquots (10 μl) of each radiolabeled reagent were retained and counted with the tissue samples for subsequent calculation of %ID/g of the tissue samples.

An identical protocol was used in seven dogs, but instead of ^{111}In-labeled polymer-modified AM-Fab, 37.5 MBq of ^{111}In-DTPA-AM-Fab (250 μg) was administered and used as positive controls. To demonstrate that ^{111}In-DTPA-PL alone, without AM-Fab, is not an infarct-avid imaging agent, we injected approximately 18.75 MBq of ^{111}In-DTPA-$PL_{3.3kD}$ (≃0.4 mg) into three dogs with experimental myocardial infarction. The experimental protocol was the same as that described above.

Determination of the In Vivo Catabolic Byproducts

After the dogs were killed, aliquots of the injected ^{111}In-DTPA-$PL_{(3.3\text{ or }17kD)}$-AM Fab, serum and urine were obtained for characterization of the radioactive species by Ultrogel AcA-34 column (1.2 × 42 cm) chromatography. Physiologic saline was used to elute the column. One-milliliter fractions were collected. Then 10-μl aliquots from each fraction were counted in a gamma counter to determine the elution patterns of the radioactive species in the preinjection sample, blood, and urine.

Statistical Analyses

Blood activity curves for each animal were fit by applying a two-compartment model of distribution kinetics with elimination assumed to occur only from the central compartment (*22*). The parameters of the resulting bioexponential functions were estimated separately for each animal with the use of a nonlinear estimation program (*23*), then these parameters were entered into a multivariate analysis of variance (MANOVA) to account for the correlations among the parameter estimates (*24*). In the comparison among the imaging agents, the Bonferroni method was used to provide multiple comparisons protection (*25*). Data in the form of samples normalized to %activity/g of the 1-min blood sample were fit, then the two resulting amplitudes were divided by their sum (and multiplied by 100) to yield %total blood activity at time 0 for each animal. Due to the resulting linear constraint on the amplitudes (their sum = 100), only the two rate constants and one amplitude for the slow (elimination) component were employed in the MANOVA.

Ex vivo counts of myocardial samples for each preparation of radiolabeled AM-Fab were grouped according to the percent of normal ^{201}Tl uptake for the sample. Thallium-201 uptake was expressed as 0%–20%, 21%–40%, 41%–60%, 61%–80%, 81%–100%, and >100% of mean normal myocardial ^{201}Tl activity. Thus, the uptake data for the imaging agents was classified in a two-way factorial design for ANOVA (analysis of variance) with four imaging-agents groups and six thallium-uptake groups. Since the Levene test revealed unequal variances, the logarithms of the counting data (in the form of %ID/g of tissue) were analyzed to stabilize the variances. Even after logarithmic transformation, the interaction between imaging-agents and thallium-uptake factors was significant, so one-way ANOVA was applied among imaging-agents for each thallium-uptake group separately (*26*). Again, the Bonferroni method was used to provide multiple-comparisons protection. A separate linear regression analysis in groups (imaging agents) was performed on the same logarithmic data to

confirm the monotonic uptake response to graded injury for each imaging agent and to compare the slopes among imaging agents of these response curves on the ordered category of thallium uptake (*27*). The middle of the % thallium uptake range was used as the independent variable for this analysis.

All error estimimates are standard errors of the relevant estimate, therefore, in the case of means, these are s.e.m.

RESULTS

Modification of monoclonal AM-Fab with DTPA-$PL_{(3.3 \text{ or } 17 \text{ kD})}$ via the use of n-HSS and Sephadex-G25 column centrifugation did not affect the immunoreactivity of the antibody. Unmodified AM-Fab, DTPA-PL modified AM-Fab and DTPA-$PL_{3.3 \text{ or } 17kD}$ were separated by anion exchange chromatography into 0.05 *M* phosphate (peak I, fractions 1–3, ≃85–95% of total Ab), 0.05 *M* phosphate/0.45 *M* NaCl (peak II, fractions 8 and 9, ≃10% of total Ab) and 0.05 *M* phosphate/0.95 *M* NaCl (peak III, fractions 13 and 14) fractions. Each peak was assessed for antibody activity (both direct and indirect binding), capacity to chelate ^{111}In, and by SDS-PAGE and Western blots. Peak I and II both had antimyosin antibody activity, whereas Peak III did not bind myosin by radioimmunoassay. Aliquots of Peak II and III chelated ^{111}In. Peak I did not. However, only the ^{111}In-labeled peak II component bound unequivocally to myosin, indicating that only peak II possessed both antibody activity and ^{111}In chelating capacity. Furthermore, SDS-PAGE and Western blots showed that Peak II migrated slightly slower than peak I. A single band of DTPA-PL_{17kD}-AM-Fab (Rf = 0.34) with an estimated M_r of 67 kD (i.e., 1 Fab and 1 PL_{17kD}), migrated slower than that of DTPA-$PL_{3.3 \text{ kD}}$-AM-Fab (Rf = 0.39, M_r 59 kD, i.e., 1 Fab and 2–3 $PL_{3.3kD}$) (Figure 1A). Both DTPA-PL modified AM-Fab migrated slower than DTPA-AM-Fab controls or Peak I (Rf = 0.44–0.45, M_r = 51–52 kD). The PIs of DTPA-$PL_{3.3 \text{ kD}}$- and DTPA-PL_{17kD}-AM-Fab were predominantly between 3.5 and 5 with minor bands in the higher range (which may be the residual unmodified AM-Fab contaminant). The PIs of DTPA-AM-Fab were between 6 and 9, with minor bands in the lower PI range. However, those of unmodified AM-Fab ranged between 7 and 9 (Fig. 1b). These data demonstrate dramatic changes in PIs after modification with negatively charged synthetic polymers.

The K_a of DTPA-$PL_{3.3kD}$- and DTPA-PL_{17kD}-AM Fab (0.7×10^9 and 1×10^9 liter/mole, respectively) were not significantly different from the K_a of the unmodified AM-Fab ($0.6–2.5 \times 10^9$ liter/mole) (Fig. 2). However, when cross-linkage was performed without the column centrifugation step, there was substantial loss of immunoreactivity and polymerization (data not shown).

The in vivo blood clearance curves are presented in Table 1 for comparison among the four preparations of AM-Fab. All biexponental curves fit the data adequately as confirmed by runs tests on the residuals. As can be seen, these curves are quite similar. The only significant differences were in the slow (elimination vs distribution) rate constant, lambda$_2$. The $T_{1/2}$ values corresponding to these rate constants were 347 min for DTPA-PL_{17kD}-AM-Fab, 248 min for DTPA-$PL_{3.3kD}$-AM-Fab, 182 min for DTPA-AM-Fab, and 267 min for radioiodinated AM-Fab. The 347-min slow component of elimination for DTPA-PL_{17kD}-AM-Fab was significantly different from the 182 min for DTPA-AM-Fab (p = 0.0007), and the 267-min slow component for the radioiodinated AM Fab was also significantly different from the 182 min for the conventionally ^{111}In-labeled DTPA-AM-Fab (p = 0.004). However, the blood activity values at 4 hr postintravenous administration of the radiotracers were not significantly different (Table 2).

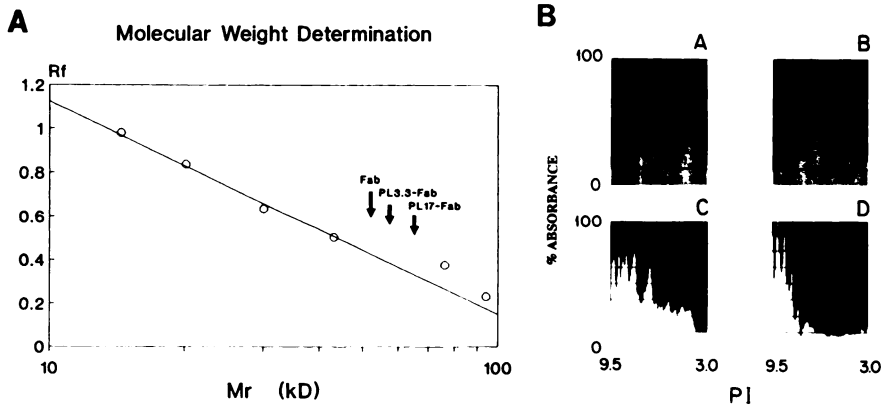

FIGURE 1. (A) Estimation of the molecular weights of AM-Fab, DTPA-AM-Fab and Peak I AM-Fab designated as Fab, and DTPA-$PL_{3.3 \text{ and } 17kD}$-AM Fab (designated as PL3.3-Fab and PL17-Fab) from SDS-PAGE using molecular weight standards of 14.4, 20.1, 30, 43, 67 and 94 kD. Rf = relative mobility determined as the ratio of the distance traversed by the sample to the distance traversed by the tracking dye in the polyacrylamide gels. (B) Absorbance profiles of the isoelectrofocusing gels of (A) DTPA-PL_{17kD}-AM-Fab, (B) DTPA-$PL_{3.3kD}$-AM-Fab, (C) DTPA-AM-Fab and (D) AM-Fab. Standards with PI range between 3.5 and 9.3 were used to calibrate the PIs of the samples.

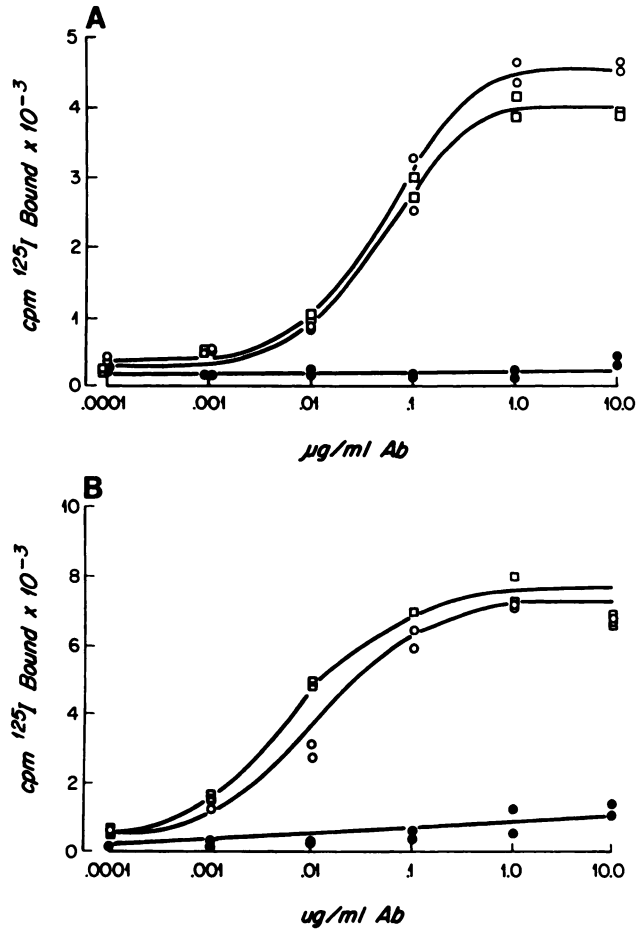

FIGURE 2. Comparison of the immunoreactivity of DTPA-$PL_{3.3kD}$-AM-Fab (○ in A) and DTPA-PL_{17kD}-AM-Fab (○ in B), control AM-Fab (□ in A and B) and nonantimyosin (anti-digoxin) monoclonal Fab (● in A and B) by solid phase radioimmunoassay. Y-axis represent cpm of ^{125}I-goat anti-murine IgG antibody bound to various preparations of antimyosin attached to cardiac myosin on the microtiter wells.

The biodistribution data (Table 2) showed that ^{111}In-DTPA-PL modified AM-Fab localized in the liver (mean %ID/g ± s.e.m., 0.020 ± 0.003 for DTPA-$PL_{3.3kD}$-AM-Fab, and 0.025 ± 0.010 for DTPA-PL_{17kD}-AM-Fab) to a significantly lower level than the conventionally ^{111}In-DTPA-AM-Fab (0.031 ± 0.009) ($p < 0.05$). The hepatic activity of radioiodinated AM-Fab was low (0.010 ± 0.004) as expected due to dehalogenation (*28*). Furthermore, the kidney cortex activity of ^{111}In-DTPA-PL_{17kD}-AM-Fab (0.015 ± 0.003) was lower than that of ^{111}In-DTPA-$PL_{3.3kD}$-AM-Fab (0.037 ± 0.022) ($p < 0.01$). Both these cortical activities were significantly lower than ^{111}In-DTPA-AM-Fab (0.173 ± 0.146) ($p < 0.001$). The radioiodine activity in the kidney cortex was also low (0.015 ± 0.005). The radioactivities in the other organs such as the spleen, kidney medulla, lungs and skeletal muscle (data not shown) showed no significant differences in the distribution of the various preparations of AM-Fab.

Another area of difference in distribution of ^{111}In-DTPA-$PL_{(3.3\ kD\ or\ 17kD)}$-AM-Fab, ^{111}In-DTPA-AM-Fab, and radioiodinated-AM-Fab is the reduction of adjacent nontarget organ background activity. Figure 3 demonstrates that ^{111}In labeled DTPA-$PL_{(3.3\text{- and }17kD)}$-AM-Fab activity in normal myocardium (81%–100% ^{201}Tl) (0.0076 ± 0.0006 [n = 164] and 0.0056 ± 0.0004 [n = 92], respectively) was significantly lower than the normal myocardial activities of conventional ^{111}In-DTPA-AM-Fab (0.0263 ± 0.0037 [n = 135]) or, ^{123}I and ^{125}I labeled AM-Fab (0.0098 ± 0.0006 [n = 256]) ($p \leq 0.001$). The myocardial background activity with ^{111}In-DTPA-PL_{17kD}-AM-Fab was significantly lower than with ^{111}In-DTPA-$PL_{3.3kD}$ AM-Fab ($p < 0.01$). The radioiodine-labeled AM-Fab activity in the normal myocardium was significantly lower than the ^{111}In-DTPA-AM-Fab activity but was still higher than either the ^{111}In-labeled $PL_{3.3kD}$- or PL_{17kD}-AM-Fab ($p \leq 0.001$). Infarct-to-normal ratios (calculated from Table 2, infarct/normal myocardial activities) were approximately 31:1 for ^{111}In-DTPA-PL_{17kD}-AM Fab, 11:1 for ^{111}In-DTPA-$PL_{3.3kD}$-AM-Fab, 8:1 for DTPA-AM-Fab and 13:1 for radioiodinated AM-Fab.

These in vitro determinations were confirmed by the in vivo immunoscintigraphic images. Figure 4 shows serial left lateral gamma images of two dogs with acute experimental myocardial infarction injected with ^{111}In-labeled DTPA-$PL_{3.3kD}$-AM-Fab (right panels) and ^{111}In-DTPA-

TABLE 1
Blood Clearance Curves for Four AM-Fab Preparations

Agent	Parameter			
	α_1	λ_1	α_2	λ_2
PL_{17kD}AM (n = 4)	25.2 ± 6.4	0.19 ± 0.08	74.8 ± 6.4	0.0020 ± 0.0002
$PL_{3.3kD}$AM (n = 6)	16.8 ± 2.7	0.14 ± 0.05	83.2 ± 2.7	0.0028 ± 0.0004
AM (n = 7)	26.3 ± 3.1	0.25 ± 0.09	73.6 ± 3.1	0.0038 ± 0.0003*
I-AM (n = 10)	27.4 ± 3.3	0.07 ± 0.02	72.6 ± 3.3	0.0026 ± 0.0002†

y = % blood activity at time $t = 0$, $y(t) = \alpha_1 e^{-\lambda_1 t} + \alpha_2 e^{-\lambda_2 t}$.
Units of α = %, $\lambda = min^{-1}$ ± s.e.m.
* $p = 0.007$ vs. PL_{17kD}AM.
† $p = 0.004$ vs. I (radioiodinated) AM.

TABLE 2
Biodistribution of ^{111}In-PL$_{3.3\text{ OR }17\text{ kD}}$-AM-Fab, ^{111}In-DTPA-AM-Fab, and Radio-iodinated AM-Fab

	% ID/g of organ ± s.e.m.					Myocardium	
			Kidney				
Sample	Liver	Spleen	Cortex	Medula	Blood	Normal	Infarct
PL$_{3.3kD}$-AM-Fab	0.020 ± 0.001*	0.010 ± 0.002	0.037 ± 0.009†	0.019 ± 0.002	0.024 ± 0.002	0.0076 ± 0.0006‡	0.0814 ± 0.0093‡
PL$_{17kD}$-AM-Fab	0.025 ± 0.005*	0.012 ± 0.003	0.015 ± 0.001†	0.014 ± 0.003	0.034 ± 0.005	0.0056 ± 0.0004‡	0.1718 ± 0.0201
DTPA-AM-Fab	0.031 ± 0.003	0.009 ± 0.001	0.173 ± 0.055	0.025 ± 0.006	0.031 ± 0.002	0.0263 ± 0.0037	0.2041 ± 0.0204
I-AM-Fab	0.010 ± 0.001*	0.009 ± 0.001	0.016 ± 0.002†	0.018 ± 0.001	0.027 ± 0.002	0.0098 ± 0.0006†	0.1335 ± 0.0187

* $p < 0.05$.
† $p < 0.01$.
‡ $p < 0.001$.
I-AM-Fab = ^{123}I or ^{125}I-labeled AM-Fab.

AM-Fab (left panels). The earliest visualization of the site of necrosis was within 30 min of the intravenous administration of ^{111}In-PL$_{3.3kD}$-AM-Fab (Fig. 4B). Within the same interval, conventional ^{111}In-DTPA-AM-Fab (n = 7) showed primarily blood-pool activity (Fig. 4A). One hour after antibody administration, the infarct visualized by ^{111}In-DTPA-PL$_{3.3kD}$-AM-Fab was unequivocally delineated (Fig. 4D), with greater target localization and less non-target (liver) activity. At 1 hr, infarct delineation by conventional ^{111}In-DTPA-AM-Fab had just begun (Fig. 4C). Comparison of the 2- and 3-hr postinjection images with ^{111}In-DTPA-PL$_{3.3kD}$-AM-Fab (Figs. 4F and 4H) and ^{111}In-DTPA-AM-Fab (Figs. 4E and 4G) shows that there was substantial hepatic activity with ^{111}In-DTPA-AM-Fab, but minimal hepatic activity and maximal infarct activity with ^{111}In-DTPA-PL$_{3.3kD}$-AM-Fab. The left lateral gamma images of the lower abdomen show that the hepatic and renal activities were minimal with negatively charged polymer-modified AM-Fab, whereas conventional ^{111}In-DTPA-AM-Fab showed both hepatic and kidney activities (data not shown). Controls (n = 3) injected with radiolabeled polymer alone showed no radiotracer localization in the infarct (Fig. 5A). The corresponding gamma images from another dog with acute experimental myocardial infarction injected intravenously with ^{111}In-DTPA-PL$_{3.3kD}$-AM-Fab is shown in Figure 5B.

Similarly, gamma images with ^{111}In-DTPA-PL$_{17kD}$-AM-Fab showed early visualization of the infarct and minimal hepatic activity (Fig. 6). The in vivo imaging data support the in vitro tissue counting studies.

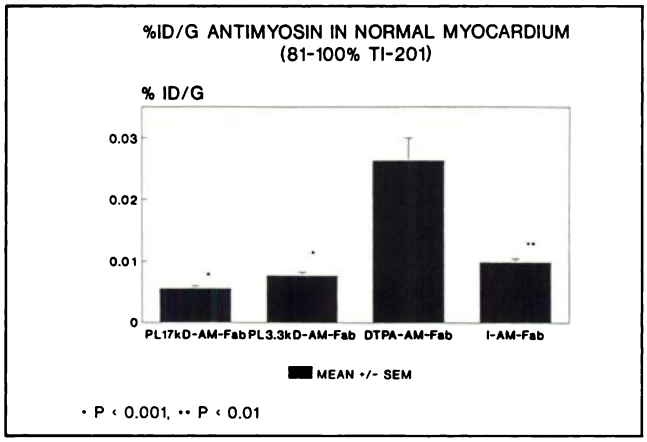

FIGURE 3. Comparison of radiotracer distribution in normal myocardium of ^{111}In-DTPA-PL$_{3.3kD}$-AM-Fab, ^{111}In-DTPA-PL$_{17kD}$-AM-Fab, ^{111}In-DTPA-AM-Fab, and radioiodinated AM-Fab, 4 hr after intravenous administration. Background myocardial activity with ^{111}In-DTPA-PL$_{3.3kD}$-AM-Fab and ^{111}In-DTPA-PL$_{17kD}$-AM-Fab was significantly lower than that with ^{111}In-DTPA-AM-Fab or radioiodinated AM-Fab ($p \leq 0.001$). Background myocardial activity of radioiodine-labeled AM-Fab was also significantly lower than that of ^{111}In-DTPA-AM-Fab ($p < 0.01$).

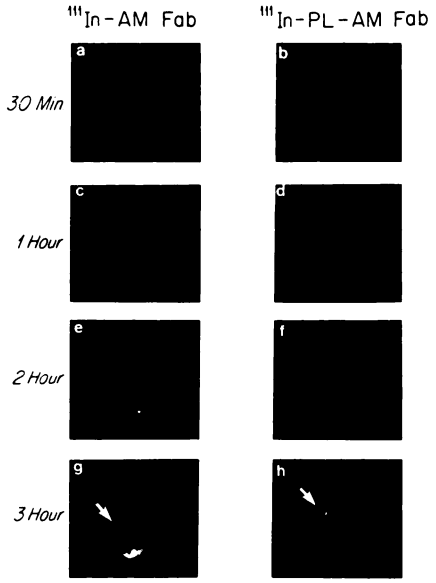

FIGURE 4. Left lateral gamma images of dogs with acute experimental myocardial infarction. (A) Image was obtained 30 min after administration of conventional ^{111}In-DTPA-AM-Fab. (B) Image was obtained 30 min after intravenous administration of ^{111}In-DTPA-PL$_{3.3kD}$-AM-Fab. (C-H) Images obtained 1, 2, and 3 hr after intravenous administration of ^{111}In-DTPA-AM-Fab and ^{111}In-DTPA-PL$_{3.3kD}$-AM-Fab, respectively. The infarcts are in the left lateral oblique position as indicated by the arrows in g and h.

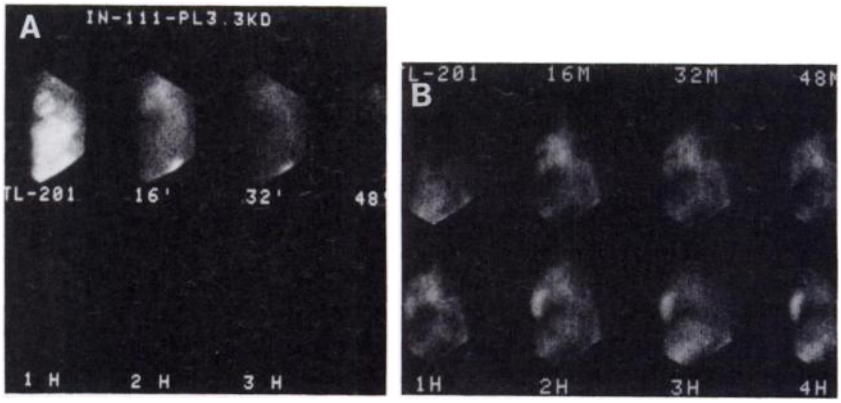

FIGURE 5. (A) Serial left lateral gamma images of a dog with experimental myocardial infarction injected with ^{111}In-DTPA-$PL_{3.3kD}$ to demonstrate that the radiolabeled polymer alone is not an infarct-avid agent. Top left panel shows the ^{201}Tl distribution image with an apical defect. The 16-, 32-, and 48-min, and 1-, 2-, and 3-hr left lateral images after ^{111}In-labeled $PL_{3.3kD}$ administration did not show infarct delineation. (B) Serial left lateral gamma images of another dog with experimental myocardial infarction injected with ^{111}In-DTPA-$PL_{3.3kD}$-AM Fab for comparison to Figure 5A. The images were acquired at the same time points as those shown above, with the exception of the 4-hr image in this figure.

To determine the fate of the radiolabeled polymer-modified AM-Fab after intravenous administration, we obtained aliquots of the antibody sample prior to in vivo administration, from the blood and urine at 4 hr after antibody administration, and then chromatographed the samples on an Ultrogel-AcA-34 column (1.5×42 cm). The preinjection sample showed only one radioactive peak corresponding to the radiolabeled ^{111}In-DTPA-PL-AM-Fab of approximate M_r of 60 kD. The serum sample also showed only one major radioactive peak corresponding to the radiolabeled AM-Fab. The urine sample, on the other hand, showed a major smaller molecular weight radioactive peak and a minor ^{111}In-DTPA-PL-AM-Fab peak (Fig. 7). These chromatographic studies showed that the ^{111}In-DTPA-PL is detached from the antimyosin either during its sojourn in the kidneys or in the urine. However, this breakdown does not appear to occur in the systemic circulation since no free ^{111}In-labeled PL peak was obtained when the serum sample was chromatographed. Figure 8 shows the relationship between ^{201}Tl distribution and various radiolabeled antimyosin myocardial uptake. At the center of infarction (%^{201}Tl from 0% to 20% and 21% to 40%), highest mean ratios of uptake were obtained with ^{111}In-DTPA-PL_{17kD}-AM-Fab. These mean ratios were significantly different from the mean ratios of uptake of ^{111}In-DTPA-$PL_{3.3kD}$-AM-Fab, ^{111}In-DTPA-AM-Fab, and ^{125}I-(^{123}I) labeled AM-Fab ($p < 0.01$). There is no statistical difference between the other groups. Table 3 shows the results of linear regression analyses of the data in Figure 10 grouped by imaging agent of uptake of the imaging agent versus ^{201}Tl uptake. The logarithm of the %ID of imaging agent per gram adequately linearized the relationship to thallium uptake (expressed as % of uptake in normal myocardium). N is the number of myocardial samples and R is the Pearson product-moment correlation coefficient. The reasonable R values (considering the large Ns) along with runs tests on residuals verified the adequacy

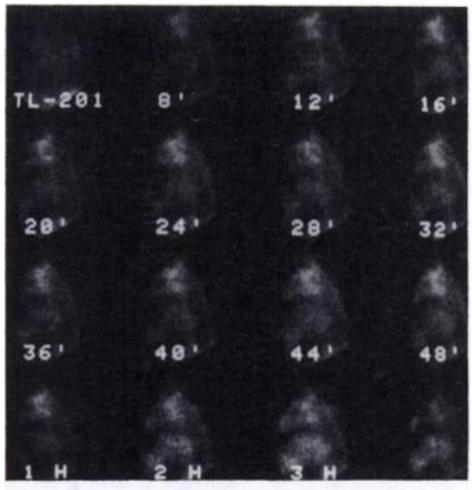

FIGURE 6. Serial left lateral gamma images of a dog with a small experimental myocardial infarction. Images were obtained at 4-min intervals starting at 8 min and continuing until 48 min (top row) and at 1, 2, 3, and 4 hr (bottom row) after intravenous injection with ^{111}In-DTPA-PL_{17kD}-AM-Fab. The ^{201}Tl distribution image (top left panel) is, however, undercontrasted.

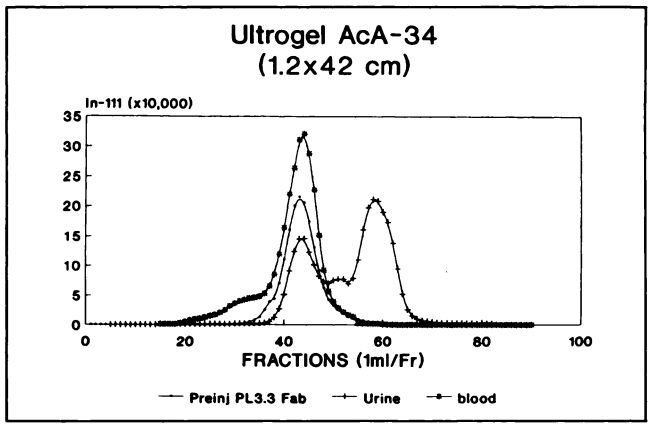

FIGURE 7. Ultrogel AcA-34 column (1.2 × 42 cm) chromatographic elution profiles of ^{111}In-DTPA-$PL_{3.3kD}$-AM-Fab, before intravenous administration (.), in canine serum (*), and in canine urine (+) obtained 4 hr after intravenous administration.

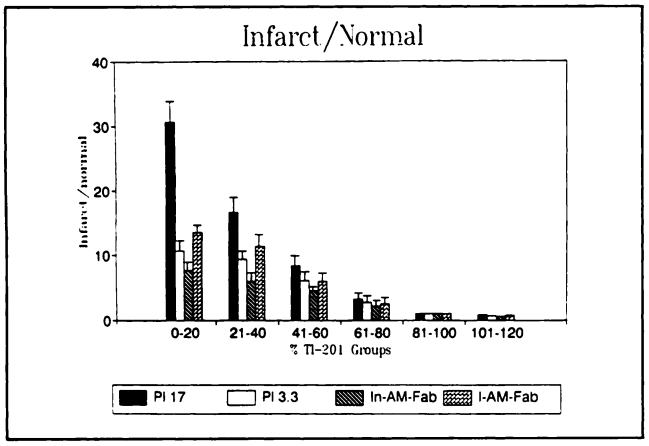

FIGURE 8. Comparison of mean target-to-normal ratios of ^{111}In-DTPA-PL$_{17kD}$-AM-Fab, ^{111}In-DTPA-PL$_{3.3kD}$-AM-Fab, ^{111}In-DTPA-AM-Fab, and radioiodinated AM-Fab in myocardial samples with 0%–20%, 21%–40%, 41%–60%, 61%–80%, 81%–100%, and >101% ^{201}Tl distribution. Myocardial tissues samples with 81%–100% ^{201}Tl distribution were used to derive at the normal myocardial activities for calculating the infarct-to-normal ratio.

of the linear curve fits. Clearly, the slope of the ^{111}In-DTPA-PL$_{17kD}$-AM-Fab curve versus the ^{201}Tl uptake is significantly steeper than that of the other curves ($p < 0.0002$ versus all other curves). All four demonstrated significant, monotonically decreasing response to diminishing injury as expected.

DISCUSSION

While the application of monoclonal antibodies as in vivo, noninvasive diagnostic and therapeutic tools has increased substantially (*29–36*), its use is still hampered by low contrast due to high background activity as well as non-target organ activities. Although the antigen recognition site is target-specific, to a large extent, its in vivo behavior is subject to nonspecific electrostatic interactions associated with the nonantigen recognition sites of the immunoglobulin molecule. One approach to modifying the in vivo properties of the antibody is to use smaller fragments such as the Fab (*37*) and F(ab')$_2$ (*38*), which lack the Fc receptor binding portion of the molecule. Since these fragments can be eliminated by excretion, they have faster blood clearance rates. Despite the increased clearance rates, however, since most antibodies are basic (positively charged) proteins, and most cells possess negatively charged cell surface structures (*1–3*), there could be weak ionic interaction between the antibodies and the cell surface. This interaction could increase the propensity for antibodies being phagocytosed by the reticuloendothelial cells of the liver, or bound nonspecifically to the highly negatively charged glomerular basement membranes of the kidneys (*39*). However, if the antibody molecules were to be modified to carry a large negative charge away from the antigen binding site, then the nonspecific ionic interactions may be decreased. The preliminary results which indicated the feasibility of this approach have been reported (*40*). The concentration of antibody required to label 18.75 MBq of ^{111}In in the preliminary study (*40*) was 25–50 times greater than the antibody concentration used in the present study to label 37.5 MBq of ^{111}In. Thus, the modified method for covalent coupling of DTPA-PL$_{(3.3 \text{ or } 17 \text{ kD})}$ to AM-Fab via the use of a carrier, n-hydroxy sulfosuccinamide, provided substantial improvement for preparation of ^{111}In-DTPA-PL-AM-Fab with very high specific activity (~50–100 mCi/mg or 1,875–3,750 MBq/mg).

In the present study, polylysine of starting molecular weights of 3.3 and 17 kD were used as examples of a small synthetic polymer and another with approximately five times the size. Larger polymers which had been prepared in our previous report were not tested (*10*). We assume that larger polymers of molecular weights 55 kD or greater will definitely slow the blood clearance of these polymer modified AM-Fab, since the size of DTPA-PL$_{55kD}$-AM-Fab would be larger than that of antimyosin F(ab')$_2$ fragments (M_R ~ 100,000kD).

Our study demonstrated that antimyosin modified to carry a large negative charge appears to enhance myocardial infarct visualization by reducing non-specific sequestration and accelerating and maintaining specific (target) localization. The enhanced target visualization is due to the reduction in background activity, probably resulting from the repulsion of negatively charged antibodies by negatively charged cell surfaces. The normal myocardial activity was decreased to 0.0056 ± 0.0004 and 0.0076 ± 0.0006 with PL$_{17kD}$ and PL$_{3.3kD}$ modified AM-Fab, respectively, from 0.0263 ± 0.0037 and 0.0098 ± 0.0006 with conventional ^{111}In-DTPA-AM-Fab and radioiodine-labeled AM-Fab, respectively ($p \leq 0.001$). This translates into 4.7 and 3.5 times higher normal myocardial activity with the conventional ^{111}In-DTPA-AM-Fab than with PL$_{17kD}$ and PL$_{3.3kD}$ modified AM-Fab, respectively. Additionally, because the affinity of antimyosin ($K_a = 5 \times 10^8$ L/M) (*11*) for myosin is stronger than the weak ionic forces of repulsion, charge-modified antimyosin can still bind avidly to its homologous antigen, which becomes

TABLE 3
Results of Linear Regression Analyses

Agent	Parameter a	b	R	N
PL$_{17kD}$AM	−0.69	−0.0168 ± 0.0007	0.83	254
PL$_{3.3kD}$AM	−0.96	−0.0131 ± 0.0006*	0.74	398
AM	−0.78	−0.0137 ± 0.0005†	0.76	654
I-AM	−0.66	−0.0123 ± 0.0009*	0.57	382

y = % ID. $\log_{10}(y) = a + bx$.
x = % of normal thallium.
* $p = 0.0001$ vs. PL$_{17kD}$AM.
† $p = 0.0002$ vs. PL$_{17kD}$AM.

exposed to the extracellular fluid after the development of holes in necrotic myocytes. Therefore, higher target-to-non-target ratios can be achieved. Although conventional ^{111}In-DTPA-AM-Fab has been reported to show uptake ratios as high as 30:1 (*41*), the mean uptake ratio in tissue samples with 0–20% ^{201}Tl distribution was 16.7 ± 1.1 (mean ± s.e.m.), whereas the mean uptake ratio of ^{111}In-DTPA-PL_{17kD}-AM-Fab in tissue samples with 0%–20% ^{201}Tl activity was approximately 31:1 (Fig. 8). The reason for the lower mean uptake ratio with ^{111}In-DTPA-$PL_{3.3kD}$-AM-Fab in the same ^{201}Tl distribution range is not clear. This increase in the target-to-background ratios should improve sensitivity and specificity for target localization and visualization.

The renal cortical activities also decreased by 4.6–11.2 times with PL-modified AM-Fab than with the conventional ^{111}In-AM-Fab. The radioiodinated AM-Fab renal activity was similar to the polymer-modified AM-Fab activities. However, the lower radioiodine activity in the cortex appears to be due to dehalogenation (*28*). Although the ^{111}In-DTPA-PL-modified antibody activity in the liver is significantly different from the liver activity of the conventional ^{111}In-labeled AM-Fab ($p < 0.05$), the difference may appear to be small when the comparisons were made on a per gram of liver basis. However, since the average weight of the liver of a 20-kg dog is approximately 450 g, the total average liver activities with ^{111}In-PL_{17kD} and ^{111}In-$PL_{3.3kD}$-AM-Fab would be about 9% and 11% ID, respectively, and the total liver activity with the conventional ^{111}In-labeled AM Fab would be about 14%ID. A decrease in the liver activity of ≃5 and 3%ID from a high of 14% with conventional ^{111}In-labeled AM-Fab to 9 and 11%ID with ^{111}In-PL_{17kD}- and ^{111}In-$PL_{3.3kD}$-AM-Fab, respectively, must be considered as highly relevant in the reduction of non-specific liver activities relative to visualization by gamma imaging.

Furthermore, because charge-modified antibodies can provide radiolabeled preparations with very high specific activity (15–30 MBq/8 μg protein), it should be possible to use substantially less antibody than is now being administered in clinical studies (*5–9*). In our study, ≃3.75 MBq of ^{111}In were radiolabeled to 1–2 μg of AM-Fab. Each animal was injected with ≃8–16 μg of DTPA-PL-modified AM Fab. Therefore, a clinical dose of 67.5 MBq (*5*) would require less than 30–40 μg of negatively charge-modified AM-Fab. Charge-modified antibodies would also reduce non-target organ activity, which could reduce the radiation burden to the patient. This reduction in radiation burden (nonspecific activity) should, in turn, permit administration of a higher dose of ^{111}In, which should provide greater photon flux, allowing images to be recorded in a shorter interval. Yet an increase in the dose of radioactivity need not be at the expense of an increase in the dose of antibody; the high specific activity of radiolabeled charge-modified molecules would permit the administration of a smaller amount of xeno-antibody protein. Whether the reduction in the amount of antibody to be injected would be an advantage in every type of tumor imaging is not certain due to reports of clinical studies where non-target organ activities were significantly decreased by co-injection of large doses of cold antibody (*33*). However, there appears to be distinct advantage in the detection and visualization of experimental myocardial necrosis as shown in this study using negatively charge-modified AM-Fab. Nevertheless, the reduction of administered xeno-proteins should reduce the incidence of anti-murine antibody response that frequently occurs in oncologic, diagnostic, and therapeutic applications of murine monoclonal antibodies (*42–44*).

ACKNOWLEDGMENTS

This work was supported in part by grant 1R01 CA50505-01A1 from the National Cancer Institute, the US/USSR Exchange Program in Cardiovascular Research—Myocardial Metabolism, the National Institutes of Health, and Centocor, Malvern, PA..

REFERENCES

1. Silva Filho FC, Santos ABS, de Carvalho TMU, de Souza W. Surface charge of resident, elicited and activated mouse peritoneal macrophages. *J Leukocyte Biol* 1987;41:143–149.
2. Levine S, Levine M, Sharp KA, Brooks DE. Theory of the electrokinetic behavior of human erythrocytes. *Biophys J* 1983;42:127–135.
3. Gallagher JE, George G, Brody AE. Sialic acid mediates the initial binding of positively charged inorganic particles to alveolar macrophage membranes. *Am Rev Respir Dis* 1987;135:1345–1352.
4. Eichmann K, Lackland H, Hood L, Krause RM. Induction of rabbit antibody with molecular uniformity after immunization with Group C streptococci. *J Exp Med* 1970;131:207–221.
5. Khaw BA, Yasuda T, Gold HK, et al. Acute myocardial infarct imaging with Indium-111-labeled monoclonal antimyosin Fab. *J Nucl Med* 1987;28:1671–1678.
6. Frist W, Yasuda T, Segall G, et al. Non-invasive detection of human cardiac transplant rejection with indium-111 antimyosin (Fab) imaging. *Circulation* 1987;76(suppl):V81–V85.
7. Yasuda T, Palacios IF, Dec GW, et al. Indium-111-monoclonal antimyosin antibody imaging in the diagnosis of acute myocarditis. *Circulation* 1987;76:306–311.
8. Johnson LL, Seldin DW, Becker LC, et al. Antimyosin imaging in acute transmural myocardial infarctions: results of a multicenter clinical trial. *J Am Coll Cardiol* 1989;13:27–35.
9. Braat SH, De Zwaan C, Teule J, Heidendal G, Wellens HJ. Value of indium-111-monoclonal antimyosin antibody for imaging in acute myocardial infarction. *Am J Cardiol* 1987;60:725–726.
10. Torchilin VP, Klibanov AL, Nossiff ND, et al. Monoclonal antibody modification with chelate-linked high-molecular-weight polymers: major increases in polyvalent cation binding without loss of antigen binding. *Hybridoma* 1987;6:229–240.
11. Khaw BA, Mattis JA, Melincoff G, Strauss HW, Gold HK, Haber E. Monoclonal antibody to cardiac myosin: imaging of experimental myocardial infarction. *Hybridoma* 1984;3:11–23.
12. Hnatowich DJ, Layne WW, Childs RL, et al. Radioactive labeling of antibody: a simple and efficient method. *Science* 1983;220:613–615.
13. Krejcarek GE, Tucker KL. Covalent attachment of chelating groups to macromolecules. *Biochem Biophys Res Comm* 1977;77:581–585.
14. Habeeb AFSA. Determination of free amino groups in proteins by trinotrobenzenesulfonic acid. *Anal Biochem* 1966;14:328–336.
15. Papisov MI, Maksimenko AV, Torchilin VP. Optimization of reaction conditions during enzyme immobilization on soluble carboxy-containing carriers. *Enzyme Micro Technol* 1985;7:11–16.
16. van Heyningen V, Brock DJH, van Heyningen S. A simple method for ranking the affinities of monoclonal antibodies. *J Immunol Methods* 1983;62:147–153.
17. Greenwood FC, Hunter WM. The preparation of ^{131}I-labeled human growth hormone of high specific radioactivity. *Biochem J* 1963;89:114–123.

18. Salacinski PRP, McLean C, Sykes JEC, Clement-Jones VV, Lowry PJ. Iodination of proteins, glycoproteins, and peptides using a solid phase oxidizing agent, 1,3,4,6-tetrachloro-3a,6a-diphenyl glycoluril (Iodogen). *Anal Biochem* 1981;117:136–146.
19. Khaw BA, Strauss HW, Cahill SL, Soule HR, Edgington T, Cooney J. Sequential imaging of indium-111-labeled monoclonal antibody in human mammary tumors hosted in nude mice. *J Nucl Med* 1984;25:592–603.
20. Williamson AR. Isoelectrofocusing of immunoglobulins. In: Weir IDM, ed. *Handbook of experimental immunology.* Oxford: Blackwell Scientific Publishing, 1978:9.1–9.31.
21. Laemmli UK. Cleavage of structural proteins during the assembly of the head of bacteriophage T4. *Nature* 1970;227:680–685.
22. Rowland M, Tozer TN. *Clinical pharmacokinetics: concepts and applications.* Philadelphia, London: Lea and Febiger, 1989:300–304.
23. Dixon WJ, Brown MB, Engleman L, Hill MA, Jennrich RI. BMDP Statistical Software Manual (to accompany the 1988 software release). Program PAR, volume 1, p. 389.
24. ibid. Program P4V, volume 2, p. 1045.
25. Morrison DF. *Multivariate statistical methods.* New York: McGraw-Hill; 1976:33–34.
26. Dixon WJ, Brown MB, Engleman L, Hill MA, Jennrich RI. BMDP Statistical Software Manual (to accompany the 1988 software release). Program P7D, volume 1, p 187.
27. ibid. Program P1R, volume 2, p. 843.
28. Khaw BA, Cooney J, Edgington T, Strauss HW. Differences in experimental tumor localization of dual-labeled monoclonal antibody. *J Nucl Med* 1986;27:1293–1299.
29. Keenan AM, Colcher D, Larson SM, Schlom J. Radioimmunoscintigraphy of human colon cancer xenografts in mice with radioiodinated monoclonal antibody B72.3. *J Nucl Med* 1984;25:1197–1203.
30. Wahl RL, Parker CW, Philpott GW. Improved radioimaging and tumor localization with monoclonal F(ab')$_2$. *J Nucl Med* 1983;24:316–325.
31. Carrasquillo JA, Abrams PG, Schroff RW, et al. Effect of antibody dose on the imaging and biodistribution of indium-111-9.2.27 anti-melanoma monoclonal antibody. *J Nucl Med* 1988;29:39–47.
32. Keenan AM, Weinstein JN, Mulshine JL, et al. Immunolymphoscintigraphy in patients with lymphoma after subcutaneous injection of indium-111-labeled T101 antibody. *J Nucl Med* 1987;28:42–46.
33. Carrasquillo JA, Bunn Jr PA, Keenan AM, et al. Radioimmunodetection of cutaneous T-cell lymphoma with ^{111}In-labeled T101 monoclonal antibody. *N Engl J Med* 1986;315:673–680.
34. Pimm MV, Perkins AC, Armitage NC, Baldwin RW. The characteristics of blood-borne radiolabels and the effect of anti-mouse IgG antibodies on localization of radiolabeled monoclonal antibody in cancer patients. *J Nucl Med* 1985;26:1011–1023.
35. Epenetos AA, Britton KE, Mather S, et al. Targeting of iodine-123-labelled tumour-associated monoclonal antibodies to ovarian, breast, and gastrointestinal tumours. *Lancet* 1982;2:999–1004.
36. Taylo A, Milton W, Eyre H, et al. Radioimmunodetection of human melanoma with indium-111-labeled monoclonal antibody. *J Nucl Med* 1988;29:329–337.
37. Porter RR. The hydrolysis of rabbit gamma-globulin and antibodies with crystalline papain. *Biochem J* 1959;73:119–126.
38. Edelman GM, Marchalonis JJ. Preparation of antigens and antibodies. *Methods Immunol Immunochem* 1967;1:422–423.
39. Kanwar YS, Farquhar MG. Presence of heparan sulfate in the glomerular basement membrane. *Proc Natl Acad Sci U S A* 1979;76:1303–1307.
40. Khaw BA, Torchilin VP, Klibanov AL, et al. Modification of monoclonal antimyosin antibody: enhanced specificity of localization and scintigraphic visualization in acute experimental myocardial infarction. *J Mol Cell Cardiol* 1989;21(suppl I):31–35.
41. Khaw BA, Gansow O, Brechbiel MW, O'Donnell SM, Nossiff N. Use of isothiocyanatobenzyl-DTPA derivatized monoclonal antimyosin Fab for enhanced in vivo target localization. *J Nucl Med* 1990;31:311–217.
42. Schroff RW, Foon KA, Beatty SM, Oldham RK, Morgan AC. Human antimurine immunoglobulin responses in patients receiving monoclonal antibody therapy. *Cancer Res* 1985;45:879–885.
43. Powell MC, Perkins AC, Pimm MV, et al. Diagnostic imaging of gynecologic tumors with the monoclonal antibody 791T/36. *Am J Obstet Gynecol* 1987;157:28–34.
44. Rosen ST, Zimmer AM, Goldman-Leikin R, et al. Radioimmunodetection and radioimmunotherapy of cutaneous T-cell lymphomas using an ^{131}I-labeled monoclonal antibody: an Illinois cancer council study. *J Clin Oncol* 1987;5:562–573.

EDITORIAL

Optimizing Antibodies for Use in Nuclear Medicine

Monoclonal antibodies (Mab) by virtue of their unique in vitro avidity for their antigen have been considered particularly attractive as selective carriers of diagnostic/therapeutic agents in vivo. This expectation is based on the fact that Mab (a) show high specificity and affinity for their intended target, (b) are generally nontoxic, and (c) can transport such agents. Their application to both diagnosis—labeled with ^{123}I or ^{131}I (*1–6*), ^{99m}Tc (*6,7*) and ^{111}In (*6,8–12*)—and therapy—labeled with the β-emitters ^{131}I (*13–17*), ^{186}Re (*18*), ^{90}Y (*19, 20*), and ^{67}Cu (*21*) and the α-emitters ^{211}At (*22–24*) and ^{212}Bi (*25–27*)— is the focus of attention in many nuclear medicine research facilities.

In all of these studies, the basic assumption continues to be that radiolabeled Mab have a role in radioimmunodiagnosis (RID) and radioimmunotherapy (RIT). How justifiable is this assumption? Certainly, several characteristics (e.g., the low percent injected dose per gram of target tissue (≤0.01%), low tumor-to-normal-tissue ratios, slow clearance, nonuniform distribution within the tumor, long biologic half-life that may be unsuitable for short-lived isotopes) could lead one to conclude that antibodies do not possess the intrinsic qualities necessary for their utilization in RID and RIT. In fact, the early enthusiasm of a decade ago has been dampened with some investigators questioning the very future of Mab in nuclear medicine (*28,29*). Despite various opinions on the subject (*30–35*), it is clear that there is a pressing need to enhance the diagnostic and/or therapeutic potential of radiolabeled Mab while maintaining their immunointegrity and minimizing structural/conformational changes that might limit their uptake and retention within the intended target.

A review of the nuclear medicine literature on radiolabeled antibodies indicates that in general there is no methodical examination of cause and effect with respect to the various inadvertent modifications that antibodies undergo during radiolabeling. Most studies have been limited to finding a technique to radiolabel the Mab with the radionuclide of interest, examining its in vitro immunoreactiv-

Received May 21, 1991; accepted May 21, 1991.

For reprints contact: Amin I. Kassis, PhD, Harvard Medical School, Shields Warren Radiation Laboratory, 50 Binney St., Boston, MA 02115.